

VERY BLUE *UV*-CONTINUUM SLOPES β OF LOW LUMINOSITY $Z \sim 7$ GALAXIES FROM WFC3/IR: EVIDENCE FOR EXTREMELY LOW METALLICITIES?¹

R. J. BOUWENS^{2,3}, G. D. ILLINGWORTH², P. A. OESCH⁴, M. TRENTI⁵, M. STIAVELLI⁶, C. M. CAROLLO⁴, M. FRANX³, P. G. VAN DOKKUM⁷, I. LABBÉ⁸, D. MAGEE²

Draft version October 30, 2018

ABSTRACT

We use the ultra-deep WFC3/IR data over the HUDF and the Early Release Science WFC3/IR data over the CDF-South GOODS field to quantify the broadband spectral properties of candidate star-forming galaxies at $z \sim 7$. We determine the *UV*-continuum slope β in these galaxies, and compare the slopes with galaxies at later times to measure the evolution in β . For luminous $L_{z=3}^*$ galaxies, we measure a mean *UV*-continuum slope β of -2.0 ± 0.2 , which is comparable to the $\beta \sim -2$ derived at similar luminosities at $z \sim 5 - 6$. However, for the lower luminosity $0.1L_{z=3}^*$ galaxies, we measure a mean β of -3.0 ± 0.2 . This is substantially bluer than is found for similar luminosity galaxies at $z \sim 4$, just 800 Myr later, and even at $z \sim 5-6$. In principle, the observed β of -3.0 can be matched by a very young, dust-free stellar population, but when nebular emission is included the expected β becomes ≥ -2.7 . To produce these very blue β 's (i.e., $\beta \sim -3$), extremely low metallicities and mechanisms to reduce the red nebular emission seem to be required. For example, a large escape fraction (i.e., $f_{esc} \gtrsim 0.3$) could minimize the contribution from this red nebular emission. If this is correct and the escape fraction in faint $z \sim 7$ galaxies is $\gtrsim 0.3$, it may help to explain how galaxies reionize the universe.

Subject headings: galaxies: evolution — galaxies: high-redshift

1. INTRODUCTION

The spectral properties of high-redshift galaxies must undergo dramatic changes at some point in the past, as the metallicities in these systems drop to lower values and these systems become progressively younger. In the limit of low metallicities, gas is no longer able to cool efficiently, likely resulting in massive extremely low-metallicity (or Population III) stars whose hot atmospheres are expected to result in a very hard *UV*-continuum spectrum and strong HeII 1640 emission. However, the strong UV flux coming from hot stars is expected to be largely offset by the redder nebular continuum light produced by the ionized gas surrounding these massive stars (e.g., Schaerer 2002).

The newly installed WFC3/IR camera on the Hubble Space Telescope permits us to observe faint $z \gtrsim 7$ galaxies $\gtrsim 40\times$ more efficiently than before, providing us with our most detailed look yet at the *UV* light and spectral properties of $z \gtrsim 7$ galaxies. Already $\gtrsim 25$ likely $z \sim 7-8$ galaxies have been identified in the early WFC3/IR

data over the Hubble Ultra Deep Field (HUDF: Oesch et al. 2009b; Bouwens et al. 2009b; McLure et al. 2009; Bunker et al. 2009), and $\gtrsim 20$ $z \sim 7$ candidate galaxies in the WFC3/IR Early Release Science (ERS) observations over the CDF-South (R.J. Bouwens et al. 2009, in prep).

Here we take advantage of these early WFC3/IR observations to study the spectral properties of candidate $z \sim 7$ galaxies. Our principal focus will be on the slope of $z \sim 7$ galaxy spectra in the *UV*-continuum – since this slope is the primary observable we can derive from the available broadband imaging data with WFC3. The *UV*-continuum slope β ($f_\lambda \propto \lambda^\beta$: e.g., Meurer et al. 1999) provides us with a powerful constraint on the age, metallicity, and dust content of high-redshift galaxies; it has already been the subject of much study at $z \sim 3 - 6$ (Lehnert & Bremer 2003; Stanway et al. 2005; Yan et al. 2005; Bouwens et al. 2006; Hathi et al. 2008; see Bouwens et al. 2009a for a systematic study at $z \sim 2 - 6$) and even at $z \sim 7$ (Gonzalez et al. 2009) using NICMOS data.

Throughout this work, we quote results in terms of the luminosity $L_{z=3}^*$ Steidel et al. (1999) derived at $z \sim 3$: $M_{1700,AB} = -21.07$. We refer to the HST F606W, F775W, F850LP, F105W, F125W, and F160W bands as V_{606} , i_{775} , z_{850} , Y_{105} , J_{125} , and H_{160} , respectively, for simplicity. Where necessary, we assume $\Omega_0 = 0.3$, $\Omega_\Lambda = 0.7$, $H_0 = 70$ km/s/Mpc. All magnitudes are in the AB system (Oke & Gunn 1983).

2. OBSERVATIONAL DATA

Our primary dataset is the ultra deep WFC3/IR data over the HUDF and the wide-area WFC3/IR ERS observations over the CDF-South (PI O'Connell: GO 11359). The HUDF data permit us to identify lower luminosity $z \sim 7$ galaxies and quantify their properties (e.g., Oesch et al. 2009b), while the ERS data permit us to do the same for more luminous $z \sim 7$ galaxies.

¹ Based on observations made with the NASA/ESA Hubble Space Telescope, which is operated by the Association of Universities for Research in Astronomy, Inc., under NASA contract NAS 5-26555. These observations are associated with programs #11563, 9797.

² UCO/Lick Observatory, University of California, Santa Cruz, CA 95064

³ Leiden Observatory, Leiden University, NL-2300 RA Leiden, Netherlands

⁴ Institute for Astronomy, ETH Zurich, 8092 Zurich, Switzerland

⁵ University of Colorado, Center for Astrophysics and Space Astronomy, 389-UCB, Boulder, CO 80309, USA

⁶ Space Telescope Science Institute, Baltimore, MD 21218, United States

⁷ Department of Astronomy, Yale University, New Haven, CT 06520

⁸ Carnegie Observatories, Pasadena, CA 91101, Hubble Fellow

For our HUDF dropout selections, we make use of the v1.0 reductions of the HUDF ACS data (Beckwith et al. 2006) rebinned on a $0.06''$ -pixel scale, and our own reduction of the HUDF09 WFC3/IR data over the HUDF (Bouwens et al. 2009b; Oesch et al. 2009b). The optical ACS imaging over the HUDF reach to 29.4, 29.8, 29.7, and 29.0 AB mag (5σ : $0.35''$ -diameter apertures) in the B_{435} , V_{606} , i_{775} , z_{850} bands, respectively, while the near-IR WFC3/IR data reach to 28.8, 28.8, and 28.8 (5σ : $0.35''$ apertures) in the Y_{105} , J_{125} , and H_{160} bands, respectively. The PSF FWHMs are $\sim 0.10''$ for the ACS data and $\sim 0.16''$ for the WFC3/IR data.

For our dropout selections over the WFC3/IR ERS fields, we make use of our own reductions of the available ACS/WFC data over the GOODS fields (Bouwens et al. 2006, 2007). Our reductions reach to 28.0, 28.2, 27.5, and 27.4 in the B_{435} , V_{606} , i_{775} , z_{850} , respectively (5σ : $0.35''$ apertures). This is similar to the GOODS v2.0 reductions, but reach ~ 0.1 - 0.3 mag deeper in the z_{850} -band due to the inclusion of the SNe follow-up data (Riess et al. 2007). Our reductions of the WFC3/IR ERS data was performed using the same procedures as we used on the HUDF09 WFC3/IR data. These data reach to 27.7 and 27.4 in the J_{125} and H_{160} bands, respectively (5σ : $0.35''$ apertures).

3. RESULTS

3.1. Catalog Creation

Our procedure for source detection and photometry is similar to that used in previous studies by our team (e.g., Bouwens et al. 2007, 2009a) and relies upon the SExtractor software (Bertin & Arnouts 1996) run in double image mode. Source detection is performed off the square root of χ^2 image (Szalay et al. 1999: similar to a coadded image) constructed from all images redward of the Lyman break. Colors are measured in small scalable apertures with a Kron (1980) parameter of 1.2 (typically $\sim 0.4''$ -diameter apertures). Fluxes measured in these small scalable apertures are then corrected (typically by ~ 0.4 mag) to total magnitudes using the additional flux in a larger scalable aperture (Kron parameter of 2.5).

3.2. $z \sim 7$ z -dropout selection

For our lower-luminosity $z \sim 7$ z -dropout selection, we use a criterion very similar that used by Oesch et al. (2009b) over the HUDF09 WFC3/IR field:

$$(z_{850} - Y_{105} > 0.8) \wedge (Y_{105} - J_{125} < 0.8)$$

Over the ERS fields, no deep WFC3 Y_{105} -band coverage is available, so we make use of the following criterion (R.J. Bouwens 2009, in prep):

$$(z_{850} - J_{125} > 0.8) \wedge (J_{125} - H_{160} < 0.3)$$

Sources are required to be undetected ($< 2\sigma$) in all bands blueward of the break (and also undetected [$< 1.5\sigma$] in no > 1 bands) to ensure that our selections are largely free of lower redshift contaminants. Sources must be detected at $\geq 5.5\sigma$ in the J_{125} band to ensure that $z \sim 7$ candidates in our sample correspond to real sources.

3.3. UV -continuum slope Measurements

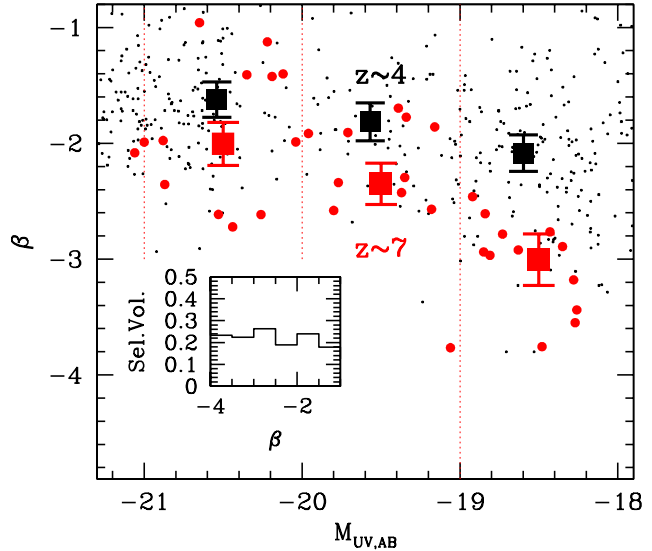


FIG. 1.— UV -continuum slope β versus absolute UV magnitude. The red circles show the β determinations and absolute magnitudes (derived from the $J_{125} - H_{160}$ colors and $\frac{1}{2}(J_{125} + H_{160})_{AB}$ magnitudes, respectively) for individual $z \sim 7$ galaxies in our HUDF09 and ERS selections. The large red squares (with 1σ error bars) represent the mean values in 1-mag bins (dotted lines). The black points correspond to the β determinations at $z \sim 4$ (Bouwens et al. 2009a). The β 's for lower luminosity galaxies at $z \sim 7$ (red circles) are much bluer (by $\Delta\beta$ of ~ 1) than those derived at $z \sim 4$ (a 4σ difference). (inset) The relative volumes available for selecting galaxies with various β 's using our HUDF09 z -dropout criterion (see §3.4). These volumes do not depend significantly on β , demonstrating that the blue β 's observed for faint $z \sim 7$ galaxies is not a selection effect.

The UV -continuum slopes β we estimate for sources in our $z \sim 7$ z -dropout sample are derived from the broad-band color $J_{125} - H_{160}$ as

$$\beta = 4.29(J_{125} - H_{160}) - 2.00 \quad (1)$$

The J_{125} and H_{160} bands here probe rest-frame $\sim 1550\text{\AA}$ and $\sim 1940\text{\AA}$, respectively, for the typical $z \sim 7$ z -dropout candidate in our sample, and are not affected by Ly α emission or IGM absorption (in contrast to the Y_{105} -band). The above equation is derived assuming a flat spectrum source with no absorption lines (found to work very well by Meurer et al. 1999).

In Figure 1, we show the β determinations for $z \sim 7$ z -dropout candidates versus luminosity. Both our ultra-deep HUDF09 and wide-area ERS selections are included, as are the $z \sim 4$ selections from Bouwens et al. (2009a). The trend of β with luminosity is illustrated with the large squares. The difference between $z \sim 7$ and $z \sim 4$ is striking.

Use of the photometry from Oesch et al. (2009b), McLure et al. (2009), or Bunker et al. (2009) for our $z \sim 7$ sample yield very consistent colors and similarly blue (or even bluer) β 's. In addition, use of a consistent $0.7''$ -diameter aperture for the color measurements yield equally blue β 's (albeit with larger random uncertainties, due to the use of larger apertures).

3.4. Consideration of Possible Selection Biases

The distribution of β 's derived for sources in our $z \sim 7$ sample can be affected by the selection process. This effect is seen in lower redshift samples, where galaxies

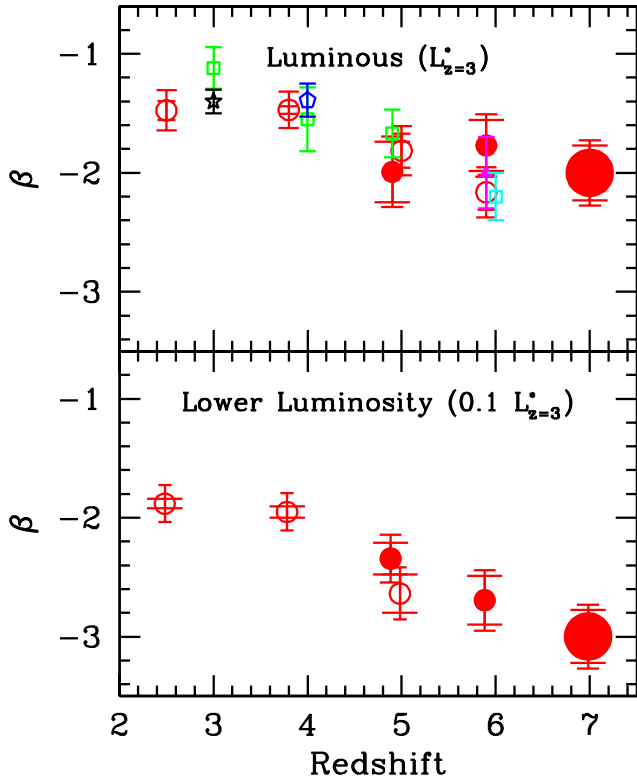


FIG. 2.— Mean UV -continuum slope measured for galaxies at $z \sim 7$ (large red circles) versus galaxies of similar luminosities at lower redshifts. The top panel shows the evolution in this slope for galaxies with a UV luminosity of $L_{z=3}^*$ (-21 AB mag) and the bottom panel shows this evolution for UV luminosities of $0.1L_{z=3}^*$ (-18.5 AB mag). The determinations of Bouwens et al. (2009a) based upon ACS+NICMOS data are shown with the open red circles. The short error bars are the random errors while the longer error bars also include possible systematic errors (e.g., see Bouwens et al. 2009a). We also show β determinations by Stanway et al. (2005: *cyan square*), Ouchi et al. (2004: *blue pentagon*), Adelberger & Steidel (2000: *black star*), and Hathi et al. (2008: *green open squares*). Note the dramatic change in β in the ~ 800 Myr from $z \sim 7$ to $z \sim 4$ for lower luminosity galaxies.

with bluer β 's have larger selection volumes than galaxies with redder β 's. To determine the importance of such effects, we constructed models with various β distributions, added galaxies with these distributions to the observational data, and then attempted to reselect these galaxies using the selection criteria in §3.2 to estimate the effective selection volume versus β . We modelled the pixel-by-pixel profiles of the sources using similar luminosity $z \sim 4$ B -dropouts from the Bouwens et al. (2007) HUDF sample, but scaled in size (physical) as $(1+z)^{-1}$ to match the observed size-redshift relationship (Oesch et al. 2009c; Ferguson et al. 2004; Bouwens et al. 2004).

The selection volumes derived from these simulations are shown in the inset to Figure 1. Encouragingly, these volumes show only a modest dependence upon the input β for the range $-4 < \beta < -1$, and so selection biases are minimal.

3.5. Low-redshift Comparison Samples

To interpret the β 's we derive from our $z \sim 7$ z -dropout selections, we compare them with the β 's found for similar luminosity galaxies at $z \sim 4 - 6$. Bouwens et al. (2009a) provide determinations of these slopes as a func-

tion of luminosity at $z \sim 2 - 6$. The β measurements at $z \sim 4$ are also shown in Figure 1 for comparison.

We can take advantage of the very deep, high-quality WFC3/IR data to obtain self-consistent determinations of these slopes at $z \sim 5-6$. The $z \sim 5$ V and $z \sim 6$ i -dropouts over the HUDF09 and GOODS ERS data are selected in the same way as in Bouwens et al. (2007; see also Giavalisco et al. 2004; Beckwith et al. 2006), except that at $z \sim 6$ we also require galaxies to satisfy the criterion ($z_{850} - J_{125} < 0.6$). At $z \sim 5$ and $z \sim 6$, the β 's are estimated based upon the $z_{850} - (Y_{105} + J_{125})/2$ and $Y_{105} - (2J_{125} + H_{160})/3$ colors, respectively, which are a good match in rest-frame wavelength to the $J_{125} - H_{160}$ colors used to estimate β at $z \sim 7$. The conversion formulas we use are

$$\beta = 4.07(z_{850} - (Y_{105} + J_{125})/2) - 2.00 \quad (z \sim 5) \quad (2)$$

$$\beta = 3.78(Y_{105} - (2J_{125} + H_{160})/3) - 2.00 \quad (z \sim 6) \quad (3)$$

In Figure 2, we plot these β determinations as a function of redshift, for both luminous L^* galaxies and lower luminosity galaxies.

3.6. $z \sim 8$ Comparison Sample

Faint $z \sim 8$ Y_{105} -dropout candidates in the HUDF09 WFC3/IR data (Bouwens et al. 2009b) also have very blue $J_{125} - H_{160}$ colors, again suggesting β 's of ~ -3 . We decided not to consider this sample here because the J_{125} -band flux can be affected by Lyman series absorption and Ly α emission at $z > 8.1$, and hence the results would be less robust.

4. DISCUSSION

Before discussing the extraordinarily blue UV -continuum slopes $\beta \sim -3$ found for lower luminosity galaxies at $z \sim 7$, we first consider the relatively luminous $L_{z=3}^*$ galaxy candidates. These sources have measured β 's of -2 , which is similar to that observed for luminous galaxies at $z \sim 3 - 6$ (Figure 2). Such slopes can be fit by a moderately young, subsolar ($0.2 Z_{\odot}$) stellar population, with a maximum $E(B - V)$ of ~ 0.05 (Calzetti et al. 2000 extinction law; see also Bouwens et al. 2009a).

The lower luminosity ($0.1L_{z=3}^*$) galaxy candidates at $z \sim 7$, by contrast, have observed β 's of -3.0 ± 0.2 . This is much bluer than for luminous $z \sim 7$ galaxies (by $\Delta\beta \sim 1$) and also much bluer than is found at $z \sim 5 - 6$ (Figures 1-2). This makes these galaxies of great interest since they are likely to be even younger, more metal poor, and dust-free than any galaxies known.

This is not a selection effect (§3.4), and cannot be attributed to Ly α emission contributing to the broadband fluxes. Ly α does not move into the J_{125} -band (used to estimate β) until $z \gtrsim 8.1$, and $\lesssim 10\%$ of our z -dropout sample extends to $z > 8$.

An AGN contribution seem similarly unlikely, given the rarity of AGN signatures in faint Lyman-Break and Ly α -emitter samples (e.g., Nandra et al. 2002; Ouchi et al. 2008).

What then is the explanation for the very blue β 's? We explore several possibilities:

4.1. Standard stellar population models

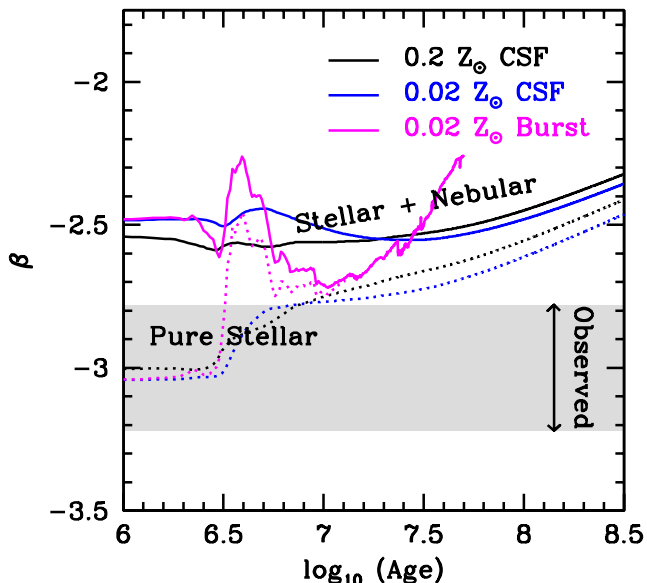


FIG. 3.— UV -continuum slope β we would expect for $z \sim 7$ galaxies as a function of age for constant star formation (CSF) models and an instantaneous burst (Schaerer 2002). The gray band denotes the observed mean β and its uncertainty. The slopes β derived from the stellar light (dotted lines) and the stellar + nebular light (solid lines) are shown. While it is in principle possible to obtain β 's of -3 with standard low metallicity ($\geq 0.02 Z_{\odot}$) models, including the nebular emission associated with hot stars make the predicted β 's ≥ -2.7 and hence too red.

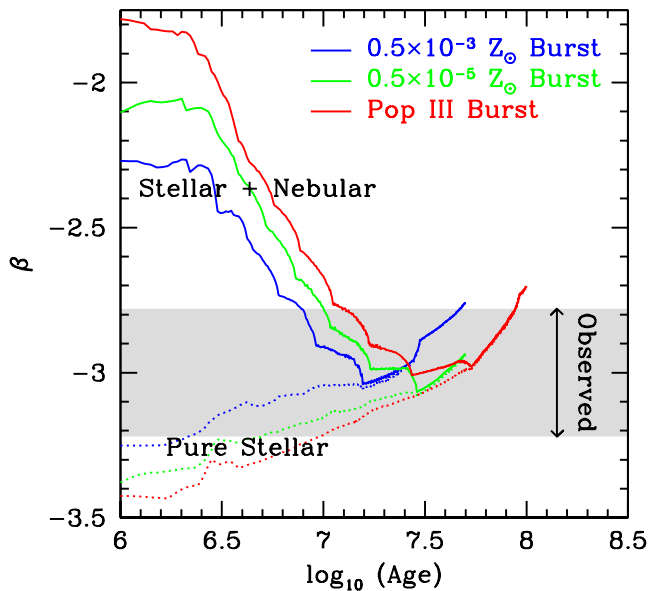


FIG. 4.— UV -continuum slope β Schaerer (2003) calculated as a function of age for instantaneous burst models for different metallicities. Both the slopes β derived from the stellar light (dotted lines) and the stellar + nebular light (solid lines) are shown. The pure stellar light (dotted lines) has very blue UV -continuum slopes β 's ($\beta \lesssim -3$) for all the low metallicity cases considered here. Changing the IMF does not appear to change the conclusion here in any significant way. Of course, these same hot low metallicity stars also ionize the gas around them, thus producing a substantial amount of redder nebular continuum light. This makes the total SED of a galaxy much redder in general, and in the calculations by Schaerer (2003) shown here, β never becomes bluer than -3.0 .

A first question is whether it is possible to obtain a β of ~ -3 using standard stellar population models (e.g., Leitherer et al. 1999; Bruzual & Charlot 2003). The answer is that it is possible, but only for very young (< 5 Myr) star-forming systems (see Figure 3). However, to do so ignores the nebular continuum emission from the ionized gas around the young stars. Including this nebular continuum emission can redden the observed β by as much as $\Delta\beta \sim 0.5$.

Figure 3 also shows the β 's predicted for several low metallicity ($0.02 Z_{\odot}$ and $0.2 Z_{\odot}$) starbursts, as a function of age for the Schaerer (2002) stellar population models (which – like *Starburst99* Leitherer et al. 1999 – include a nebular contribution). In the best cases, the models predict β 's as blue as -2.7 , which is redder than what we observe in our faint samples.⁹ This would suggest that lower metallicities are needed since the standard Leitherer et al. (1999) or Bruzual & Charlot (2003) stellar population models do not produce blue enough colors to match those found in our lower luminosity $z \sim 7$ sample. Of course, the significance of this result is only modest ($< 1.3\sigma$), but the similarly blue colors observed for $z \sim 8$ selections (Section 3.6) suggest that we may want to take this finding at face value.

4.2. Extremely low metallicities ($\leq 10^{-3} Z_{\odot}$)

In Figure 4 we present the β 's predicted by the Schaerer (2003) stellar population models (which conveniently provide predictions at extremely low metallicities) as a function of age for instantaneous bursts assuming a metallicity of $0.5 \times 10^{-3} Z_{\odot}$, $0.5 \times 10^{-5} Z_{\odot}$, and zero (population III).¹⁰ From the figure, it is clear that the nebular component contributes significantly to the total light output from $\lesssim 10^{-3} Z_{\odot}$ stellar populations.

While initially somewhat red due to the nebular contribution, the predicted β 's for these ultra-low metallicity models become much bluer at ages > 10 Myr, eventually reaching β 's of -3 . Such metallicities and ages are not necessarily unreasonable for lower luminosity galaxies at $z \sim 7$, and therefore at least one possible explanation for the very blue β 's in our selection is that the metallicities for galaxies in our sample may be $\lesssim 10^{-3} Z_{\odot}$.

The above explanation may explain some of the very blue galaxies in our selection, but given that $\beta \sim -3$ only for a limited period (10-30 Myr after a burst), it seems unlikely to be the general explanation (unless updated models revise the theoretical SEDs).

4.3. Top-heavy IMF

One seemingly attractive explanation for the very blue β 's observed is through a top-heavy IMF, since galaxy stellar populations would be weighted towards massive, blue stars. The difficulty with this explanation is that these same massive stars are extraordinarily efficient at ionizing the gas around them – resulting in substantial nebular emission and leaving the galaxy with a net β no bluer (and likely redder) than the young (< 1 Myr) bursts

⁹ To match the wavelength baseline for β measured here, we added -0.1 to the β 's (1300-1800Å baseline) tabulated in the Schaerer (2002, 2003).

¹⁰ The use of instantaneous burst models allows us to explore the most extreme cases. Other models (τ , inverse τ , CSF) produce comparable β 's.

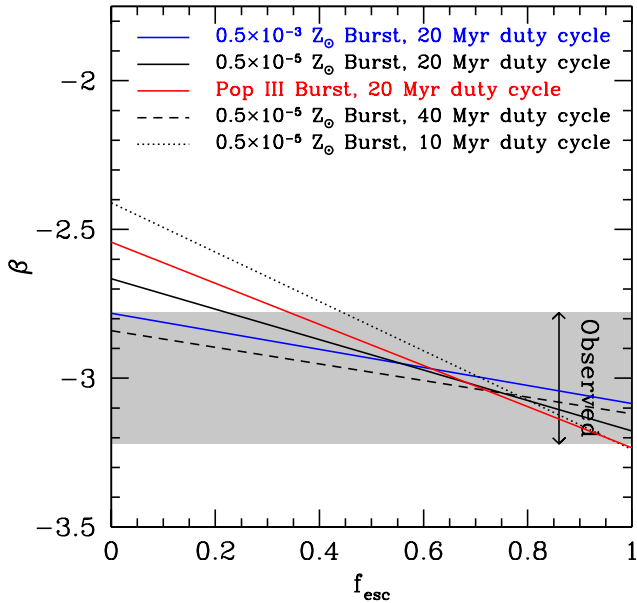


FIG. 5.— Mean UV-continuum slopes β 's predicted for high-redshift galaxy samples versus the escape fraction f_{esc} . The predictions are made using the Schaerer (2003) stellar population models (including nebular emission) for metallicities of $< 10^{-3} Z_{\odot}$. Galaxies are assumed to be observed at some random point during their star formation histories and to experience instantaneous bursts of star formation every 10-40 Myr (the dashed, solid, and dotted lines give the average β for the first 10, 20, and 40 Myr, respectively, of the instantaneous burst). For $f_{esc} = 1$, all of the ionizing radiation from a galaxy escapes into the IGM and hence does not contribute to ionizing the gas within a galaxy (and hence the contribution from nebular continuum emission to the total light is minimal). On the other hand, for $f_{esc} \sim 0$ (preferred in some simulations: e.g., Gnedin et al. 2008), the ionizing radiation from the hot stars does not make it out of galaxies – resulting in substantial nebular continuum emission (see Figure 4) and hence a much redder β . Perhaps the very blue β 's observed (shaded gray region) could indicate that the escape fraction is larger at $f_{esc} \gtrsim 0.3$ than what has commonly been considered?

shown in Figures 3-4 (see also discussion in Leitherer & Heckman 1995).

4.4. Minimizing nebular emission

A significant obstacle to matching the very blue β 's observed is the red nebular emission associated with hot, ionizing stars. The nebular contribution could be reduced in a number of ways, by changes to the ionization parameter, metallicity, geometry, etc. Assessing the impact of such changes would benefit from further detailed modelling. However, we should emphasize that regardless of changes to the nebular contribution very low metallicity models (or very young ages) appear to be needed to match the very blue β 's observed.

4.5. Changes in Escape Fraction?

One possibility that we have explored to reduce the nebular emission contribution is if the ionizing radiation leaks directly into the IGM (e.g., due to the effect of SNe on the galaxies' ISM, possibly from a top-heavy IMF: Trenti & Shull 2009). We consider such a possibility schematically in Figure 5, showing the time-averaged β 's expected for stellar populations of various metallicities as a function of the escape fraction f_{esc} of ionizing photons into the IGM. For f_{esc} of unity, we simply recover the β 's from the pure stellar SEDs and for f_{esc} of zero, we recover the stellar + nebular SEDs. For fractional f_{esc} , we interpolate between the two extremes. The time-averaged β 's used for Figure 5 is based upon those presented in Figure 4.

Comparing the predicted β 's with that observed (grey-shaded region: Figure 5), we see that $f_{esc} \gtrsim 0.3$ would permit us to easily match the observations. Such an escape fraction is significantly higher than the $\sim 10\%$ frequently assumed in calculations assessing the sufficiency of galaxies to reionize the universe. Since most of the luminosity density at $z > 7$ comes from low luminosity galaxies, the estimated number of ionizing photons in the $z > 7$ universe could increase by factors of $\gtrsim 3$. Such a large change could provide the needed photons to reionize the universe, providing a resolution to the current debate (e.g., Bouwens et al. 2008; Oesch et al. 2009a, 2009b; McLure et al. 2009; Bunker et al. 2009; Gonzalez et al. 2009; Ouchi et al. 2009; Pawlik et al. 2009).

5. SUMMARY

The strikingly blue UV-continuum slopes β 's seen at lower luminosities in candidate $z \sim 7$ galaxies (also apparent in the Bouwens et al. 2009b $z \sim 8$ sample) indicate that we are now beginning to explore a regime where the nature of galaxies and their stellar populations are undergoing a dramatic change. These results raise many as yet unanswered questions, but could be heralding the transition from the first stars and youngest objects within the first 400 Myr at $z \gtrsim 10$ to the galaxies that dominate the universe for the next 2 Gyr and provide clues as to the source of photons that reionize the universe.

We thank Daniel Schaerer for helpful conversations. We are grateful to all those at NASA, STScI and throughout the community who have worked so diligently to make Hubble the remarkable observatory that it is today. We acknowledge the support of NASA grant NAG5-7697 and NASA grant HST-GO-11563.01.

REFERENCES

- Adelberger, K. L. & Steidel, C. C. 2000, ApJ, 544, 218
 Beckwith, S. V. W., et al. 2006, AJ, 132, 1729
 Bertin, E. and Arnouts, S. 1996, A&AS, 117, 39
 Bouwens, R. J., Illingworth, G. D., Blakeslee, J. P., Broadhurst, T. J., & Franx, M. 2004, ApJ, 611, L1
 Bouwens, R. J., Illingworth, G. D., Blakeslee, J. P., & Franx, M. 2006, ApJ, 653, 53
 Bouwens, R. J., Illingworth, G. D., Franx, M., & Ford, H. 2007, ApJ, 670, 928
 Bouwens, R. J., Illingworth, G. D., Franx, M., & Ford, H. 2008, ApJ, 686, 230
 Bouwens, R. J., et al. 2009a, ApJ, 705, 936
 Bouwens, R. J., et al. 2009b, ApJ, in press, arXiv:0909.1803
 Bruzual, G., & Charlot, S. 2003, MNRAS, 344, 1000
 Bunker, A., et al. 2009, MNRAS, in press, arXiv:0909.2255
 Calzetti, D., Armus, L., Bohlin, R. C., Kinney, A. L., Koornneef, J., & Storchi-Bergmann, T. 2000, ApJ, 533, 682
 Ferguson, H. C. et al. 2004, ApJ, 600, L107
 Giavalisco, M., et al. 2004a, ApJ, 600, L93
 Gnedin, N. Y., Kravtsov, A. V., & Chen, H.-W. 2008, ApJ, 672, 765

- Gonzalez, V., Labbe, I., Bouwens, R., Illingworth, G., Franx, M., Kriek, M., Brammer, G. 2009, *ApJ*, submitted, arXiv:0909.3517
- Hathi, N. P., Malhotra, S., & Rhoads, J. E. 2008, *ApJ*, 673, 686
- Kron, R. G. 1980, *ApJS*, 43, 305
- Lehnert, M. D. & Bremer, M. 2003, *ApJ*, 593, 630
- Leitherer, C., & Heckman, T. M. 1995, *ApJS*, 96, 9
- Leitherer, C., et al. 1999, *ApJS*, 123, 3
- McLure, R., et al. 2009, *MNRAS*, in press, arXiv:0909.2437
- Meurer, G. R., Heckman, T. M., & Calzetti, D. 1999, *ApJ*, 521, 64
- Nandra, K., Mushotzky, R. F., Arnaud, K., Steidel, C. C., Adelberger, K. L., Gardner, J. P., Teplitz, H. I., & Windhorst, R. A. 2002, *ApJ*, 576, 625
- Oesch, P. A., et al. 2009a, *ApJ*, 690, 1350
- Oesch, P.A., et al. 2009b, *ApJ*, in press, arXiv:0909.1806
- Oesch, P.A., et al. 2009c, *ApJ*, in press, arXiv:0909.5183
- Oke, J. B., & Gunn, J. E. 1983, *ApJ*, 266, 713
- Ouchi, M., et al. 2004, *ApJ*, 611, 660
- Ouchi, M., et al. 2008, *ApJS*, 176, 301
- Ouchi, M., et al. 2009, *ApJ*, 706, 1136
- Pawlik, A. H., Schaye, J., & van Scherpenzeel, E. 2009, *MNRAS*, 394, 1812
- Riess, A. G., et al. 2007, *ApJ*, 659, 98
- Schaerer, D. 2002, *A&A*, 382, 28
- Schaerer, D. 2003, *A&A*, 397, 527
- Stanway, E. R., McMahon, R. G., & Bunker, A. J. 2005, *MNRAS*, 359, 1184
- Steidel, C. C., Adelberger, K. L., Giavalisco, M., Dickinson, M., and Pettini, M. 1999, *ApJ*, 519, 1
- Szalay, A. S., Connolly, A. J., & Szokoly, G. P. 1999, *AJ*, 117, 68
- Trenti, M., & Shull, M. 2009, *ApJ*, submitted, arXiv:0905.4505
- Yan, H., et al. 2005, *ApJ*, 634, 109